



OPEN Preferable effect of CTLA4-Ig on both bone erosion and bone microarchitecture in rheumatoid arthritis revealed by HR-pQCT

Naoki Iwamoto^{1✉}, Ko Chiba², Shuntaro Sato³, Shigeki Tashiro³, Kazuteru Shiraishi², Kounosuke Watanabe², Nozomi Ohki⁴, Akitomo Okada⁵, Tomohiro Koga¹, Shin-ya Kawashiri^{1,6}, Mami Tamai¹, Makoto Osaki² & Atsushi Kawakami¹

This exploratory study aimed to examine the impact of abatacept treatment on bone structure in patients with rheumatoid arthritis (RA) using high-resolution peripheral quantitative computed tomography (HR-pQCT). RA patients initiating either abatacept or newly introduced csDMARDs were enrolled in this prospective, non-randomized, two-group study. Bone structure in the 2nd and 3rd metacarpal heads was assessed using HR-pQCT at 0, 6, and 12 months after enrollment. Synovitis was evaluated using musculoskeletal ultrasound and MRI. The adjusted mean between-group differences (abatacept–csDMARDs group) were estimated using a mixed-effect model. Thirty-five patients (abatacept group: $n = 15$; csDMARDs group: $n = 20$) were analyzed. Changes in erosion volume, depth and width were numerically smaller in the abatacept group compared to the csDMARDs group (adjusted mean between-group differences: -1.86 mm^3 , -0.02 mm , and -0.09 mm , respectively). Over a 12-month period, 5 erosions emerged in the csDMARDs group, while only 1 erosion appeared in the abatacept group. Compared to csDMARDs, abatacept better preserved bone microarchitecture; several components of bone microarchitecture were significantly worsened at 6 months in the csDMARDs group, but were not deteriorated at 6 months in the abatacept group. Changes in synovitis scores were similar between the two treatment groups. Our results indicate that abatacept prevented the progression of bone erosion including new occurrence, and also prevented worsening of bone strength independently with synovitis compared to csDMARDs including MTX. Thus, abatacept treatment may provide benefits not only in inhibiting the progress of bone erosion but also in preventing bone microarchitectural deterioration.

Keywords Rheumatoid arthritis, CTLA4-Ig, Abatacept, csDMARDs, Bone microarchitecture, Bone erosion, Hr-pQCT

Abbreviations

RA	Rheumatoid arthritis
HR-pQCT	High-resolution peripheral quantitative computed tomography bDMARDs: biological disease-modifying antirheumatic drugs
cs	Conventional synthetic
CTLA-4	Cytotoxic T-lymphocyte-associated antigen4
BMD	Bone mineral density
RANKL	Receptor activator of nuclear factor-kappa B ligand

¹Division of Advanced Preventive Medical Sciences, Department of Immunology and Rheumatology, Nagasaki University Graduate School of Biomedical Sciences, 1-7-1 Sakamoto, Nagasaki 852-8501, Japan. ²Department of Orthopedic Surgery, Nagasaki University Graduate School of Biomedical Sciences, 1-7-1 Sakamoto, Nagasaki 852-8501, Japan. ³Clinical Research Center, Nagasaki University Hospital, 1-7-1 Sakamoto, Nagasaki 852-8501, Japan. ⁴Department of Radiological Sciences, Nagasaki University Graduate School of Biomedical Sciences, 1-7-1 Sakamoto, Nagasaki 852-8501, Japan. ⁵Department of Rheumatology, National Hospital Organization Nagasaki Medical Center, Kubara 2-1001-1, Omura, Nagasaki 856-8562, Japan. ⁶Center for Collaborative Medical Education and Development, Nagasaki University Institute of Biomedical Sciences, 1-7-1 Sakamoto, Nagasaki 852-8501, Japan. ✉email: naoki-iwa@nagasaki-u.ac.jp

IL	Interleukin
ACR	American College of Rheumatology
EULAR	European League against Rheumatism
RF	Rheumatoid factor
ACPA	Anti-citrullinated protein antibodies
MRI	Magnetic resonance imaging
DXA	Dual-energy X-ray absorptiometry
Tb.vBMD	Trabecular volumetric bone mineral density
BV/TV	Trabecular bone volume fraction
Tb.N	Trabecular number
Tb.Th	Trabecular thickness
Tb.Sp	Trabecular separation
JCR	Japan College of Rheumatology
US	Ultrasound
GS	Gray scale
PD	Power Doppler
MCP	Metacarpophalangeal
IP	Interphalangeal
PIP	Proximal interphalangeal
RAMRIS	Rheumatoid arthritis magnetic resonance imaging score
mTSS	Modified total sharp score
ITAC	Interferon inducible T-cell alpha chemoattractant
MIP	Macrophage inflammatory protein
DKK	Dickkopf
OPG	Osteoprotegerin
OC	Osteocalcin
OPN	Osteopontin
SOST	Sclerostin
DAS	Disease activity score
ESR	Erythrocyte sedimentation rate
CDAI	Clinical disease activity index

Rheumatoid arthritis (RA) is a systemic autoimmune disease principally effecting synovial joints and characterized by a distinctive pattern of bone and joint destruction. One of the crucial goals of treating RA is to prevent bone destruction, which can ultimately lead to joint damage and a decline in the quality of life, affecting everyday activities.

High-resolution peripheral quantitative computed tomography (HR-pQCT) is an advanced 3-dimensional imaging technique with superior sensitivity in assessing bone¹.

Due to its high resolution, HR-pQCT surpasses conventional methods such as X-ray or computed tomography in evaluating bone erosion. HR-pQCT allows independent measurement of specific parameters of bone erosion, such as width, depth, and volume, in addition to revealing the status of the bone microarchitecture. In previous studies, HR-pQCT has been used to detect peri-articular osteoporosis in RA and has provided detailed insights into the changes in bone erosion and microarchitecture throughout the clinical course of RA^{2–5}. However, few studies using HR-pQCT have focused on the association of bone structure with biological disease-modifying antirheumatic drugs (bDMARDs), and comparison with conventional synthetic (cs) DMARDs is even rarer^{6–8}.

Abatacept is a soluble fusion protein of the extracellular domain of the human cytotoxic T-lymphocyte-associated antigen 4 (CTLA-4), which inhibits the activation of T lymphocytes by binding the CD80 and CD86 on the surface of antigen-presenting cells. Clinical trials have demonstrated that abatacept exhibits efficacy similar to other bDMARDs, leading treatment guidelines to recommend it on par with other bDMARDs^{9–11}. Several large studies have demonstrated that abatacept has an inhibitory effect on bone erosion progression^{12,13}. However, in these studies only conventional image modalities such as X-ray were used to analyze the bone erosions, and comprehensive investigations linking abatacept treatment with detailed periarticular osteoporosis remain lacking, despite observations of increased bone mineral density (BMD) with abatacept treatment^{14,15}. Also, there are several subsets of CD4 T helper (Th) cells with different functions, such as Th1, Th2, Th17, and Tfh, and these have been suggested to play a role in RA activity. Indeed, the importance of these subsets was also confirmed by previously described clinical effects of abatacept. Among T-cell subsets, Th17 has been implicated in promoting bone destruction through its expression of receptor activator of nuclear factor-kappa B ligand (RANKL) via interleukin (IL)-17¹⁶. Conversely, cytokines such as IL-4 or interferon- γ that are produced by other Th subsets exert inhibitory effects on osteoclast differentiation. Consequently, the precise roles of T-cell subsets in synovitis and bone destruction in RA remain incompletely elucidated, with previous reports indicating conflicting effects on joint destruction by T-cell function or osteoclastic effects by T regs.

Thus, in this study, we used HR-pQCT to analyze the detailed changes in bone microarchitecture and other aspects of joint structure during abatacept treatment, and a multiplex assay to analyze the T-cell related factors.

Methods

Study design, patients and treatment

This study is a prospective non-randomized two-group exploratory study that assessed the association between abatacept treatment and bone microarchitecture using HR-pQCT. Patients were included who (1) fulfilled the 2010 American College of Rheumatology (ACR)/European League against Rheumatism (EULAR) classification

criteria for RA¹⁷; (2) were administered no more than 7.5 mg prednisolone equivalent per day; (3) had not received any drugs for osteoporosis; and 4) had no history of administration with biologic or targeted synthetics DMARDs. Consecutive patients who met all these requirements and in whom treatment with abatacept or one of the newly introduced csDMARDs had been planned were enrolled. All patients were enrolled at the Nagasaki University Hospital. Written informed consent which was approved by Nagasaki University Hospital Institutional Review Board (Institutional Review board approval no. 16092611) was obtained from all patients. We collected the data of all patients in each group at baseline, including age, sex, disease duration, positivity of rheumatoid factor (RF) and anti-citrullinated protein antibodies (ACPA) and concomitant medications.

Efficacy endpoints

The primary endpoint was the change from baseline in bone erosion detected by HR-pQCT in joints to be evaluated. Additionally, a co-primary endpoint was the change in bone microarchitecture. Secondary endpoints assessed through month 12 included synovitis evaluated by ultrasound; synovitis, bone erosion and osteitis assessed via magnetic resonance imaging (MRI); BMD, evaluated using Dual-energy X-ray absorptiometry (DXA); joint destruction, assessed by X-ray; serum biomarkers obtained through a multiplex bead assay; and clinical disease activity. Detailed information regarding the variables adapted to outcomes is described in the following section.

Variables to be assessed

High-resolution peripheral quantitative computed tomography

HR-pQCT (XtremeCT II, SCANCO Medical AG, Brüttisellen, Switzerland) of the second and third metacarpal bones (of the affected hand, the more severely affected hand [if both hands were affected], or the hand of the subject's dominant arm [if both hands were unaffected or affected to equal extents]) was performed at months 0, 6 and 12 and bone erosion was evaluated as described previously¹⁸. In addition to bone erosion, the following indices of bone microarchitecture were estimated using HR-pQCT: trabecular volumetric bone mineral density (Tb.vBMD), trabecular bone volume fraction (BV/TV), trabecular number (Tb.N), trabecular thickness (Tb.Th), and trabecular separation (Tb.Sp).

Ultrasound assessment

Several Japan College of Rheumatology (JCR)-certified rheumatologists who were blinded to the clinical information and laboratory data performed musculoskeletal ultrasound (US) at months 0, 6 and 12. For correction of interobserver variability, the obtained US images was also evaluated among them, and discussed to reach a consensus. A systemic multiplanar gray scale (GS) and power Doppler (PD) examination were performed in the following 22 joints: the bilateral wrists (intra-carpal, radiocarpal and ulnocarpal recesses) and finger joints including the 1st–5th metacarpophalangeal (MCP) joints, the 1st interphalangeal (IP) joint and the 2nd–5th proximal interphalangeal (PIP) joints (dorsal recess) with the same scanner (Toshiba AplioXG, Canon i800) using a multifrequency linear transducer. Each joint was given a GS and PD score from 0 to 3 according to the US findings, as described previously¹⁹.

Magnetic resonance imaging of wrists and finger joints

MRIs of the wrists and finger joints of the affected hand were acquired using 3 T system (Sigma; General Electric Medical Systems, Milwaukee, WI) with an extremity coil at months 0, 6 and 12. Coronal T1-weighted spin-echo (repetition time [TR] 450, echo time [TE] 13) and STIR (TR 3000, TE 12, T1 160) images were acquired. The images were evaluated for osteitis, bone erosion, and synovitis according to the rheumatoid arthritis magnetic resonance imaging score (RAMRIS)^{20,21}. The MRIs were scored by two independent experienced radiologists (MU, NO) who were blinded to the clinical data.

Bone mineral density measurement

DXA was performed to evaluate the BMD of the lumbar spine (L2-L4) and femoral neck at months 0, 6 and 12. A Discovery™ Wi QDR densitometer (Hologic, Bedford, MA) was used for bone densitometry. Radiographs of the thoracic and lumbar spine were taken for pre-existing vertebral fractures and new fractures at the same time as BMD measurement.

Radiographs

Radiographs of hands/wrists and feet were obtained at months 0, 6 and 12. Two readers (TK, AO) who were trained and certified by Prof. van der Heijde (Leiden University Medical Center) and blinded to the treatment and clinical status of patients independently reviewed and scored the images using the modified total Sharp score (mTSS), as described previously^{22,23}.

Multiplex bead assay

We measured the concentrations of the biomarkers using serum stored at months 0, 6 and 12. We performed a multiplex cytokine/chemokine bead assay using MILLIPEX MAP human Cytokine/Chemokine Magnetic Bead Panel 1-premixed 38 Plex (Millipore, Billerica, MA) kits as described previously²⁴. And for detection of following biomarkers related to T-cells and bone metabolism; Interferon Inducible T-Cell Alpha Chemoattractant (ITAC), macrophage inflammatory protein (MIP)-3 α , IL-21, IL-23, Dickkopf (DKK)1, osteoprotegerin (OPG), osteocalcin (OC), osteopontin (OPN) and sclerostin (SOST), the custom multiplex bead assay was performed in parallel. The biomarkers that were frequently found to be at non-detectable levels were excluded from analysis.

Clinical assessment

The patients' clinical disease activity was assessed using the disease activity score in 28 joints-erythrocyte sedimentation rate (DAS28-ESR) and Clinical Disease Activity Index (CDAI) at baseline and at 3, 6, 9 and 12 months after enrollment.

Statistical analysis

Since this was an exploratory study and there were no previous data with which to gauge a sample size, a statistical sample size calculation was not performed. Therefore, based on feasibility, we set a target sample size of 40 patients, 20 in the abatacept group and 20 in the csDMARDs group.

Firstly, we summarized and compared the baseline characteristics for each group. Continuous data were presented as mean \pm standard deviation (SD) and compared using the Wilcoxon rank-sum test. Categorical data were presented as number and percentage and compared using Fisher's exact test.

Next, we descriptively examined the actual values and changes from baseline for each outcome measure. The Adjusted mean between-group differences at each time point were estimated using a mixed-effects model. The objective variable was the change from baseline, and the fixed effects were group, time point, multiple term between group and time point, and adjustment variables including age, sex, steroid administration status, rheumatoid arthritis disease duration, ACPA, and baseline values of the outcome measures. RF was excluded from the adjusted variables because the same patients tested positive for both ACPA and RF. The random effects were the patients, and for the HR-pQCT data, which were available for each joint, the joint was also included. The between-group differences were estimated as the difference in the mean values for each group, and 95% confidence intervals were also estimated. *P*-values were calculated but not adjusted for multiplicity.

For actual value of bone microarchitecture, and biomarker analysis, normal distribution of the data was confirmed using the Kolmogorov–Smirnov test. And, The Student's paired t-test was utilized to identify statistically significant differences in the parameters of bone microarchitecture, whereas the Wilcoxon signed rank test was used for non-parametric data. For comparison of biomarker change, the Student's unpaired t-test was employed for parametric data, and the Mann–Whitney U test was used for non-parametric data. As this study is exploratory, caution should be exercised when interpreting the *P*-values. All statistical analyses were performed using R version 4.3.2 or GraphPad prism software.

Results

Patient disposition and baseline characteristics

Nineteen patients received abatacept and 22 patients received newly introduced csDMARDs in this study. Within the abatacept group, 2 patients discontinued treatment before the 6-month mark due to allergy or personal preference, and an additional 3 patients ceased abatacept therapy after 6 months due to inefficacy or adverse events (specifically, pneumonia and leukopenia). Within the csDMARDs group, 2 patients withdrew consent before the 6-month period, and an additional 6 patients discontinued treatment after 6 months: 4 due to worsening arthritis that necessitated bDMARDs and 2 due to withdrawal of consent. All other patients completed the 12-month observation period while receiving either abatacept or csDMARDs treatment. Finally, 2 patients from the abatacept group were excluded due to unanalyzable HR-pQCT results.

Our analysis thus focused on 15 patients from the abatacept group and 20 patients from the csDMARDs group who underwent HR-pQCT scans at least twice, once at baseline and again at the 6-month mark. Table 1 summarizes the baseline demographic and disease characteristics of the patients. The abatacept group exhibited higher age, longer disease duration and less concomitant oral steroid dose as compared with the csDMARDs group. Other baseline characteristics, including sex, ACPA/RF positivity and disease activity, were comparable between the two treatment groups.

	Abatacept (N = 15)	csDMARDs (N = 20)	P value
Female, n (%)	12 (80.0)	17 (85.0)	> 0.99
Age, years	73.1 \pm 8.7	63.2 \pm 9.7	0.004
Duration of RA, years	5.0 \pm 5.9	2.0 \pm 5.0	0.006
csDMARDs		MTX:18,TAC:1 SASP:1	
Concomitant MTX use, n (%)	7 (46.7)		
Concomitant oral steroid use, n (%)	4 (26.7)	7 (35.0)	0.721
Mean oral steroid dose (mg/day)	2.25 \pm 1.89	5.86 \pm 1.86	0.018
ACPA positive, n (%)	12/13 (92.0)	14/20 (70.0)	0.198
RF positive, n (%)	12/13 (92.0)	14/20 (70.0)	0.198
DAS28-ESR	5.19 \pm 1.57	5.01 \pm 1.34	0.593
CDAI	20.5 \pm 14.3	21.0 \pm 10.2	0.913

Table 1. Clinical characteristics of the study population. Data are mean \pm standard deviation (SD) unless otherwise indicated. RA rheumatoid arthritis, csDMARDs conventional synthetic disease-modifying antirheumatic drugs, MTX methotrexate, ACPA anti-citrullinated protein antibodies, RF rheumatoid factor, DAS disease activity score, ESR erythrocyte sedimentation rate, CDAI clinical disease activity index.

Changes in bone erosion

Changes in bone erosions at the 2nd and 3rd metacarpal heads were assessed by HR-pQCT. At baseline, there were 16 and 9 erosions in the abatacept and csDMARDs groups, respectively. Table 2 shows the alteration in erosion volume, as quantified by HR-pQCT. The mean change from baseline (SD) in the volume of bone erosion as measured by HR-pQCT at 12 months after initiating each treatment was -1.14 (2.49) mm^3 in abatacept group vs. -0.26 (0.9) mm^3 in the csDMARDs group (Fig. 1). After adjusting for age, sex, concomitant use of steroid, disease duration, and ACPA, the adjusted mean difference between the two groups was -1.86 mm^3 (95% CI: -4.28 , 0.56 ; $P=0.122$). Similar results were observed for the adjusted mean difference between the groups regarding the depth of bone erosion (change from baseline to month 12: -0.02 mm; 95% CI: -0.30 , 0.27 ; $P=0.890$) and width of bone erosion (change from baseline to month 12: -0.09 mm; 95% CI: -0.35 , 0.17 ; $P=0.476$).

In addition to achieving a better improvement in the mean quantification of erosion volume, the abatacept group also demonstrated a greater number of improvements in erosion volume compared to the baseline (Supplemental Table S1). In the abatacept group, 6 erosions exhibited improvement compared to baseline, whereas in the csDMARDs group only 3 erosions showed improvement. Furthermore, the csDMARDs group exhibited a higher frequency of newly appearing erosions compared to the abatacept group. Over a 12-month period, 5 erosions emerged in the csDMARDs group, while only 1 erosion appeared in the abatacept group. These findings suggest that the csDMARDs treatment may be associated with a higher risk of developing new erosions in comparison to the abatacept treatment.

Changes in bone microarchitecture

In addition to assessing bone erosion, bone microarchitecture was evaluated using HR-pQCT. Table 3 summarizes the findings regarding changes in bone microarchitecture. The mean changes (SD) in periarticular vBMD of the 2–3 metacarpal heads, as measured by HR-pQCT, were -1.63 (13.43) mg/cm^3 in the abatacept group and -5.26 (21.57) mg/cm^3 in the csDMARDs group from baseline to month 12. After adjustment, the mean difference between the two groups was 1.22 mg/cm^3 (95% CI: -7.37 , 9.81 ; $P=0.778$). Similar trends were observed in adjusted mean difference of BV/TV, Tb.N and Tb.Sp, with changes of 0.38% , $0.021/\text{mm}$, and -15.29 μm , respectively. However, there was a contrasting result for Tb.Th, where the adjusted mean difference between the two groups was -0.45 μm . Although the adjusted mean difference between two groups was not significantly different, the actual values of several components of bone microarchitectures, such as vBMD and BV/TV, significantly worsened at 6 months in the csDMARDs group (we were only able to compare mean values of each time point up to 6 months, as not all patients had completed the study by the 12-month mark), whereas in the abatacept group, there was no deterioration observed at 6 months (Fig. 2). These results suggest that abatacept shows a more favorable association with bone microarchitecture compared to csDMARDs.

Influence of ACPA titer and concomitant use of MTX in abatacept treatment

We next examined the differences in changes in bone erosion and bone microarchitecture within the abatacept group by ACPA status and concomitant use of MTX. The adjusted mean difference at 12 months between the high ACPA titer group (ACPA $>100\text{U}/\text{ml}$) and the non-high titer group was 27.51 mm^3 (95%CI: -8.68 , 64.70 ; $P=0.134$) for bone erosion and -4.03 mg/cm^3 (95% CI: -13.21 , 5.16 ; $P=0.371$) for vBMD, respectively. Regarding concomitant MTX use, the respective values were -184.6 mm^3 (95%CI: -456.0 , 87.39 ; $P=0.177$) and -3.89 mg/cm^3 (95%CI: -12.24 , 4.45 ; $P=0.343$).

Month	Abatacept (N = 15)	csDMARDs (N = 20)	Adjusted mean difference (Abatacept - csDMARDs) [95%CI], P value
	Mean change from baseline (SD)	Mean change from baseline (SD)	
Bone erosion-volume, mm^3			
6	-0.77 (2.56)	-0.36 (1.13)	-0.97 [-3.07 , 1.13], $P=0.337$
12	-1.14 (2.49)	-0.26 (0.90)	-1.86 [-4.28 , 0.56], $P=0.122$
Bone erosion-depth, mm			
6	0.03 (0.23)	-0.05 (0.14)	0.02 [-0.20 , 0.25], $P=0.830$
12	-0.04 (0.30)	-0.09 (0.18)	-0.02 [-0.30 , 0.27], $P=0.890$
Bone erosion- width, mm			
6	-0.06 (0.21)	0.01 (0.15)	-0.11 [-0.34 , 0.11], $P=0.293$
12	-0.16 (0.38)	-0.22 (0.41)	-0.09 [-0.35 , 0.17], $P=0.476$

Table 2. Change from baseline in bone erosion parameters evaluated by HR-pQCT. The adjusted mean differences at each time point were estimated using a mixed-effects model. The objective variable was the change from baseline, and the fixed effects were group, time point, multiple term between group and time point, and adjustment variables including age, sex, steroid administration status, rheumatoid arthritis disease duration, RF, and baseline values of the outcome measures. The random effects were the patients and each joint. SD standard deviation, CI confidence interval.

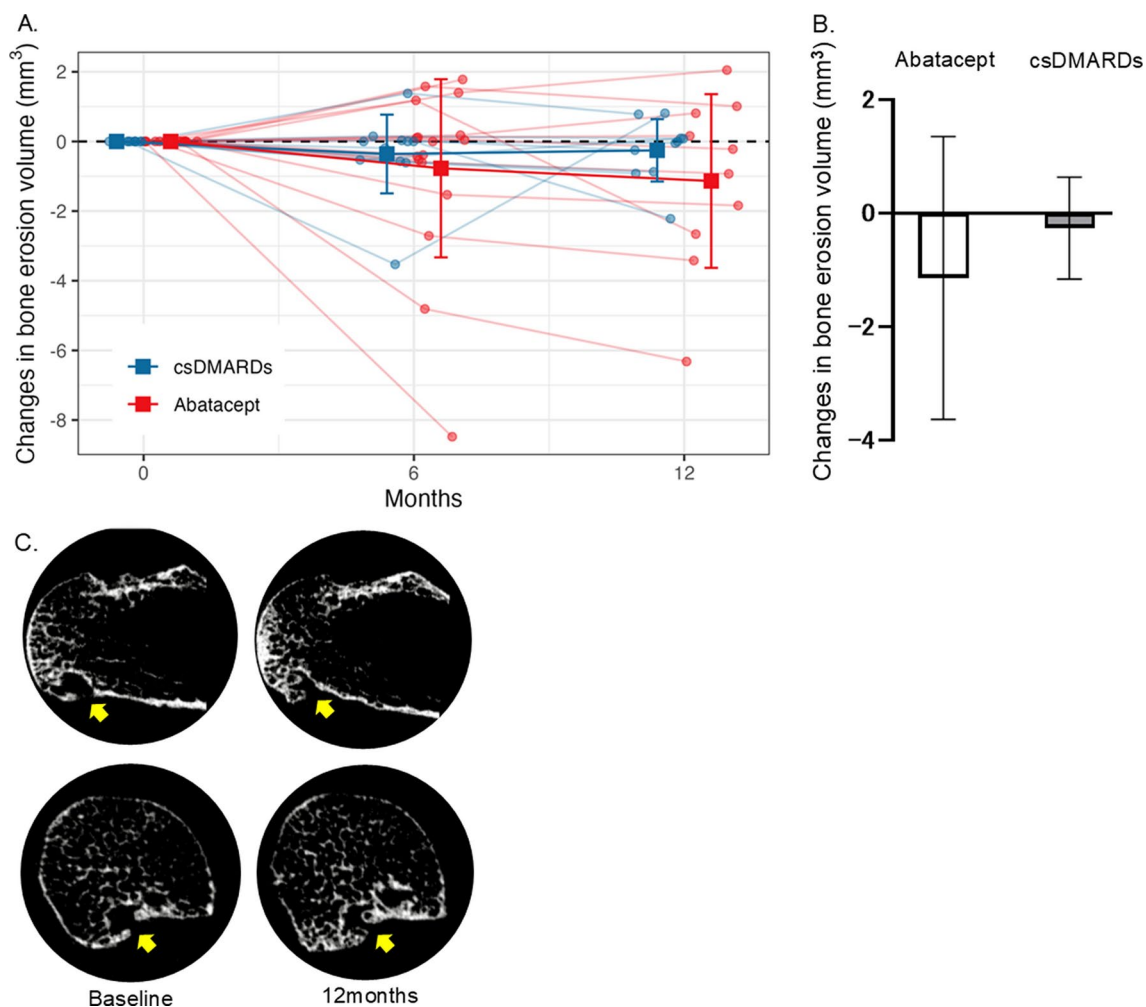


Fig. 1. (A) Time course of bone erosion volume of the 2–3 metacarpal over 12 months of abatacept and csDMARDs treatments. *Square points* and *bars* represent means and standard deviations, respectively. (B) Mean change from baseline in bone erosion volume of the 2–3 metacarpal head at 12 months. Error bars represents standard deviation. (C) Representative images of HR-pQC) of the metacarpal head in patients treated with abatacept, demonstrating improvement in erosion. Yellow allow indicate erosion. Upper row; Coronal image, Lower row; Axial image.

Clinical response

The clinical response was comparable between the two groups throughout the observation period (Table 4). In the abatacept group, the mean changes (SD) of DAS28 – ESR and CDAI from baseline to month 12 were -1.54 (1.44) and -11.65 (8.79), respectively. The corresponding values in the csDMARDs group were -1.72 (1.55) and -13.92 (11.11), respectively. The differences in adjusted mean change from baseline to month 12 between the two groups were not significant. For DAS28 – ESR, the adjusted mean difference was 0.01 (95% CI: -0.92 , 0.94; $P=0.986$). Similarly, for CDAI, the adjusted mean difference was -0.5 (95% CI: -6.09 , 5.08; $P=0.858$), indicating no significant difference between the two groups in terms of clinical response.

Synovitis and osteitis detected by US and MRI

The changes in RAMRIS total score and US synovitis score from baseline to month 12 are summarized in Table 4. Notably, both scores demonstrated improvement in both groups. The adjusted between-group differences in the change in total RAMRIS score by MRI and PD score by US from baseline to month 12 were found to be 2.12 (95%CI: -10.67 , 14.91; $P=0.740$) and 0.03 (95%CI: -3.39 , 3.45; $P=0.986$), respectively.

Radiographic progression

In addition to the synovitis and osteitis changes mentioned above, Table 4 shows the changes in radiographic bone destruction measured by mTSS throughout observation period. While no significant differences were observed, the csDMARDs group showed greater progression in bone erosion compared to the abatacept group. The mean change (SD) in total score from baseline to 12 months was -1.2 (7.0) in the abatacept group, whereas it amounted to 1.4 (1.7) in the cs DMARDs group (the adjusted between – group difference in the change in TSS from baseline to month 12 was -2.08 (95% CI: -5.41 , 1.25; $P=0.215$).

Month	Abatacept (N = 15)	csDMARDs (N = 20)	Adjusted mean difference (Abatacept – csDMARDs) [95%CI], P value
	Mean change from baseline (SD)	Mean change from baseline (SD)	
Tb.vBMD, mg/cm ³			
6	- 0.89 (10.79)	- 7.90 (19.56)	3.46 [- 3.97, 10.88], P = 0.355
12	- 1.63 (13.43)	- 5.26 (21.57)	1.22 [- 7.37, 9.81] P = 0.778
BV/TV, %			
6	- 0.15 (1.71)	- 1.15 (2.81)	0.62 [- 0.46, 1.71], P = 0.254
12	- 0.31 (1.99)	- 0.86 (2.91)	0.38 [- 0.87, 1.63], P = 0.548
Tb.N, 1/mm			
6	- 0.03 (0.10)	- 0.02 (0.08)	0.02 [- 0.02, 0.06], P = 0.368
12	- 0.01 (0.07)	- 0.01 (0.10)	0.02 [- 0.03, 0.07], P = 0.399
Tb.Sp, μm			
6	13.26 (26.26)	11.38 (37.75)	- 14.75 [- 32.49, 2.99], P = 0.101
12	15.53 (23.33)	13.44 (46.60)	- 15.29 [- 35.49, 4.91], P = 0.136
Tb.Th, μm			
6	- 0.3 (5.64)	- 3.38 (8.17)	0.88 [- 2.94, 4.70], P = 0.645
12	- 0.89 (8.02)	- 2.75 (9.10)	- 0.45 [- 4.77, 3.88], P = 0.837

Table 3. Change from baseline in bone microarchitecture parameters evaluated by HR-pQCT. The Adjusted mean differences at each time point were estimated using a mixed-effects model. The objective variable was the change from baseline, and the fixed effects were group, time point, multiple term between group and time point, and adjustment variables including age, sex, steroid administration status, rheumatoid arthritis disease duration, RF, and baseline values of the outcome measures. The random effects were the patients. *csDMARDs* conventional synthetic disease-modifying antirheumatic drugs, *Tb.vBMD* trabecular volumetric bone mineral density, *BV/TV* trabecular bone volume fraction, *Tb.N* trabecular number, *Tb. Sp* trabecular separation, *Tb.Th* trabecular thickness, *SD* standard deviation, *CI* confidence interval.

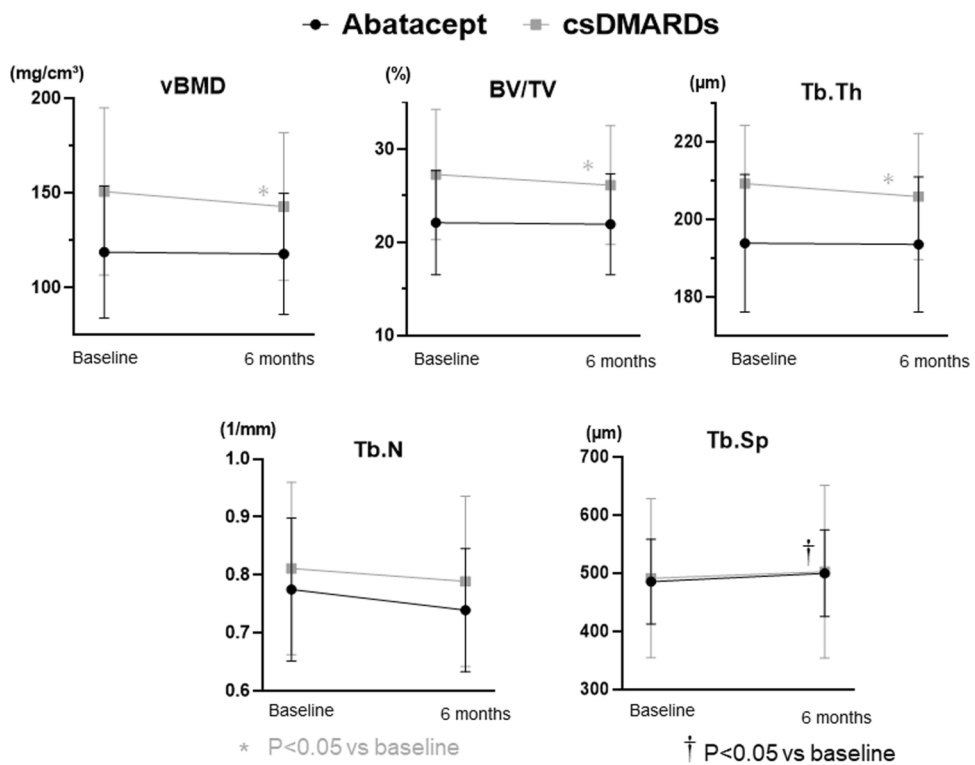


Fig. 2. Changes in bone microarchitectures of the 2–3 metacarpal over 6 months of abatacept and csDMARDs treatments. *Square points* and *bars* represent means and standard deviations, respectively. *†*p* < 0.05 vs. baseline by the Wilcoxon signed rank test.

Month	Abatacept (N = 15)	csDMARDs (N = 20)	Adjusted mean difference (Abatacept – csDMARDs) [95%CI], P value
	Mean change from baseline (SD)	Mean change from baseline (SD)	
DAS28-ESR			
6	– 1.05 (1.20)	– 1.54 (1.41)	0.35 [– 0.58, 1.28], P = 0.452
12	– 1.54 (1.44)	– 1.72 (1.55)	0.01 [– 0.92, 0.94], P = 0.986
CDAI			
6	– 10.00 (11.18)	– 12.74 (9.45)	1.66 [– 3.55, 6.86], P = 0.529
12	– 11.65 (8.79)	– 13.92 (11.11)	– 0.50 [– 6.09, 5.08], P = 0.858
PD score in both hands by musculoskeletal ultrasound			
6	– 2.9 (5.2)	– 4.2 (8.9)	– 0.65 [– 4.02, 2.72], P = 0.695
12	– 3.6 (4.3)	– 6.4 (11.7)	0.03 [– 3.39, 3.45], P = 0.986
GS + PD score in both hands by musculoskeletal ultrasound			
6	– 6.0 (9.0)	– 8.6 (16.0)	0.59 [– 6.09, 7.28], P = 0.857
12	– 6.8 (6.5)	– 10.6 (18.0)	1.50 [– 5.32, 8.33], P = 0.657
RAMRIS total score by MRI			
6	– 8.1 (11.3)	– 3.7 (13.6)	– 0.59 [– 12.54, 11.35], P = 0.921
12	– 10.2 (9.6)	– 7.6 (19.3)	2.12 [– 10.67, 14.91], P = 0.740
mTSS by X-ray			
6	0.7 (1.2)	0.9 (1.1)	0.52 [– 2.62, 3.66], P = 0.739
12	– 1.2 (7.0)	1.4 (1.7)	– 2.08 [– 5.41, 1.25], P = 0.215
Lumbar spine, %			
6	– 0.71 (2.64)	0.47 (3.67)	– 1.35 [– 5.34, 2.65], P = 0.498
12	0.17 (2.87)	1.82 (6.07)	– 1.87 [– 5.70, 1.95], P = 0.326
Femoral neck, %			
6	– 2.22 (1.93)	– 1.36 (2.53)	– 0.75 [– 3.46, 1.96], P = 0.574
12	– 2.94 (2.83)	– 0.22 (3.35)	– 2.59 [– 5.24, 0.05], P = 0.054

Table 4. Change from baseline in clinical evaluations and other secondary endpoints evaluated by other imaging modalities. The adjusted mean differences at each time point were estimated using a mixed-effects model. The objective variable was the change from baseline, and the fixed effects were group, time point, multiple term between group and time point, and adjustment variables including age, sex, steroid administration status, rheumatoid arthritis disease duration, RF, and baseline values of the outcome measures. The random effects were the patients. *csDMARDs* conventional synthetic disease-modifying antirheumatic drugs, *DAS* disease activity score, *ESR* erythrocyte sedimentation rate, *CDAI* clinical disease activity index, *PD* power Doppler, *GS* gray scale, *RAMRIS* rheumatoid arthritis magnetic resonance imaging score, *MRI* magnetic resonance imaging, *mTSS* modified total Sharp score, *BMD* bone mineral density, *DXA* Dual-energy X-ray absorptiometry, *SD* standard deviation, *CI* confidence interval.

Systemic bone mass change

The association between abatacept treatment and systemic bone metabolism was also evaluated in this study. The percent changes from baseline to 6 and 12 months in BMD of the lumbar spine and femoral neck measured by DXA are summarized in Table 4. At the 12 – month mark, there was an increase in areal BMD at the lumbar spine compared to baseline. Notably, this increase was numerically higher in the csDMARDs group compared to the abatacept group: 1.82% (6.07) vs. 0.17% (2.87), respectively. Conversely, the areal BMD at the femoral neck showed a decrease at 12 months from baseline in both groups. Similarly to the lumbar spine, the rate of decrease was lower in the csDMARDs group, which exhibited a decline of only – 0.22% (3.35), compared to the abatacept group's larger decrease of – 2.94%. After adjustment, the mean differences between the two groups were – 1.87 (95%CI: – 5.70, 1.95; $P=0.326$) in the lumbar spine and – 2.59 (95%CI: – 5.24, 0.05; $P=0.054$) in the femoral neck.

Biomarker

Changes in serum humoral factors related to inflammation, T-cells and bone metabolism were evaluable in 24 of the enrolled patients (abatacept group: $n=9$; csDMARDs group: $n=15$). For most of the evaluated humoral factors, changes over the treatment period were comparable between the abatacept and csDMARDs group, with only the osteopontin level exhibiting a significantly greater increase from baseline at both 6 and 12 months in the abatacept group compared to the csDMARDs group (Supplemental Table S2). The mean change in osteopontin level from baseline to month 12 was 383.9 pg/mL in the abatacept group, whereas that were – 273.0 pg/mL in the csDMARDs group (the between-group difference in the change in serum osteopontin levels from baseline to month 12 was 656.9 (95%CI: 163.0, 1058.0; $P<0.005$).

Discussion

In this study, HR-pQCT enabled a detailed analysis of bone structure changes during abatacept treatment in patients with rheumatoid arthritis. The findings indicate that abatacept exhibits a greater inhibitory effect on the progression of bone erosion and deterioration of bone quality compared to treatment with csDMARDs. After 1 year of treatment, the mean bone erosion volume decreased, and although not statistically significant, the reduction in erosion volume was notably greater compared to that by csDMARDs treatment. Furthermore, abatacept demonstrated superior efficacy in preventing the occurrence of new bone erosions for one year, i.e., only one new erosion was detected. Several previous researches have indicated that abatacept prevents bone erosion in RA^{12,13}. However, results of most of these studies come from radiological analyses, and conventional radiography is not sensitive enough to detect early structural change. Indeed, one study reported that the sensitivity and specificity of conventional radiography for RA patients in whom bone erosion was detected by HR-pQCT were 85% and 38%, respectively²⁵. This more precise detection method was better able to detect differences in the bone erosion progression rate between abatacept and csDMARDs compared with previous reports. Moreover, bone repair could also be observed by using HR-pQCT, mean bone erosion volume decreased with superiority in abatacept group. This result suggested that abatacept affected not only inhibition of bone erosion but also bone formation. Giovanni et al. reported that serum bone formation markers (B-ALP, PTH and P1NP) were increased during abatacept treatment²⁶. And CTLA4-Ig affect to bone formation with relation of Wnt/ β -Catenin signal have been reported²⁷.

In the present study almost all parameters of bone microarchitecture were worsened in both groups, but such worsening was less pronounced by abatacept treatment than by csDMARDs treatment. In the analysis of actual value, though the analysis could be performed up to 6 months due to treatment discontinuation, the csDMARDs group exhibited a statistically significant worsening, whereas such deterioration was not observed in the abatacept group. Periarticular osteoporosis as pre-exist of bone erosion have been reported^{28–30}. In a study that assessed the efficacy of infliximab, progression in erosions was independently associated with increased bone mineral density loss in the hands after 1 year³⁰. These results are consistent with our study, as we found that csDMARDs treatment worsened various parameters of bone microarchitecture, including vBMD, and that new bone erosion was more prevalent in the csDMARDs group compared to the abatacept group. One possible reason for these favorable effects on periarticular bone as compared to csDMARDs treatment might have been related to the actions of osteoclasts. Bozec et al. revealed that CTLA4-Ig directly inhibited osteoclast differentiation by inducing the IDO pathway,³¹ and other report revealed that interfering with intracellular calcium oscillations resulted in inhibition of osteoclast differentiation by CTLA4-Ig.³² In addition to osteoclastogenesis, an *in vivo* imaging experiment revealed that CTLA4-Ig prevented attachment of osteoclast precursor cells to bone surfaces³³. The beneficial effects of various anti-rheumatic agents on preventing deterioration of bone microarchitecture, as observed in our current study, are consistent with findings from previous research utilizing HR-pQCT. Notably, baricitinib treatment was shown to significantly enhance in trabecular vBMD⁸. In this study, thirty RA patients underwent detailed analysis of microarchitecture during 12-months baricitinib treatment. HR-pQCT analysis revealed significant improvement in the trabecular vBMD of MCP joint with a mean change of 6.11 mg hydroxyapatite/cm³. The number and size of erosion remained stable. Recent studies have reported that Jak inhibitors improve bone quality through modulation of osteoblast function. The *in vivo* study by Adam et al. revealed that JAK inhibitor increased osteoblast function, such as osteocalcin and Wnt signaling, and another study using three different types of bone loss models also reported that JAKinhibitor enhanced osteoblastic bone formation in the calcaneus distal to inflammatory synovium^{34,35}. Additionally, denosumab, a fully human monoclonal immunoglobulin G2 antibody specific to the RANKL, exhibited improvements across multiple parameters of bonemicroarchitecture compared to csDMARDs monotherapy^{3,36}. Thus, anti-rheumatic drugs improve bone microstructure through mechanisms specific to each drug. A comprehensive comparison of anti-rheumatic agents, not only focusing on bone erosion but also considering their impact on bone microarchitecture, is essential for accurately evaluating their efficacy in managing rheumatoid arthritis.

Previous clinical studies including phase 3 trials have demonstrated the superiority of abatacept over csDMARDs in regard to clinical response and synovitis^{37–39}. However, in our present study, synovitis and clinical disease activity were improved by both treatments, with csDMARDs showing slightly superior numerical efficacy. Despite adjusting for baseline characteristics in our analysis, there remains a possibility that the following factors influenced clinical outcomes and synovial inflammation—i.e., our csDMARDs patients had shorter disease duration and more concomitant use of prednisolone, which could have contributed to a good clinical response and synovitis even in the csDMARDs group.

The preventive effects against systemic bone loss, as evaluated by BMD of the lumbar spine and femoral neck, did not mirror the previous results on periarticular bone loss. The increase in BMD at the lumbar spine appeared to be numerically smaller, and the decline in BMD at the femoral neck to be greater, by abatacept treatment compared to csDMARDs treatment. These findings suggest that the impact on osteoclast activity by abatacept might be more pronounced at inflammation sites such as the periarticular region. Furthermore, considering that the loss of BMD in the femoral neck, which is predominantly composed of cortical bone, was higher in the abatacept group, the effect of abatacept may be more substantial in trabecular bone. However, because larger studies have reported an increase in BMD effects with abatacept compared to other biologic DMARDs and csDMARDs, it is essential to interpret our present results with caution^{14,15}.

Serum osteopontin level increased during abatacept treatment compared to treatment with csDMARDs. Osteopontin, a transformation-associated phosphoprotein, is intricately linked to bone metabolism and homeostasis. While there is still controversy regarding the effect of osteopontin on osteoblast, previous studies have suggested its role in promoting osteoblast proliferation and calcification induced by mechanical stress⁴⁰. Additionally, other studies reported the promotion of the adhesion of MC3T3-E1/C4 osteoblastic cell by osteopontin, and that accompanied with high expression of Runx2, osteopontin promote bone remodeling

and reduce bone loss in osteoporosis^{41–43}. Conversely, osteopontin has been implicated in enhancing osteoclastogenesis, e.g., osteopontin affects the adhesion and spread of osteoclasts through PKCa/RhoA-Rac1 signaling pathway⁴⁴. Despite its potential to enhance osteoclast function, the diverse effects of osteopontin raise the possibility that abatacept may augment bone mass through the increase of osteopontin.

Several studies reported that abatacept is more effective in ACPA high titer group as compared non-high titer group^{45,46}. To explore this in effect of bone structure, we performed subgroup analysis in abatacept group. Unlike the clinical response results, there was less improvement in bone erosion in the ACPA high-titer group. One possible reason is that RA with ACPA high-titer is prone to progressive bone destruction, so the influence of ACPA as a poor prognostic factor may be stronger than the superior efficacy of abatacept. Further analysis with a larger number of patients is needed.

There are several limitations associated with this study. The most important limitation is the small sample size and short observation period. Additionally, a number of patients were unable to undergo the third HR-pQCT (at 12 months) mainly due to changes in treatment regimen. Nonetheless, leveraging HR-pQCT enabled us to elucidate a significant deterioration in bone microarchitecture with conventional treatment over 6 months, and suggested that abatacept is preferable to csDMARDs in terms of minimizing bone destruction. When planning this study, we calculated our sample size based on an expectation that the number of erosions would be similar between the treatment groups. However, the actual number of patients with erosions in the csDMARDs group was smaller than anticipated, which is one reason why the sample size was smaller and there was no significant change regarding bone structure between treatment groups. Another potential limitation is the variation in background characteristics among the treatment groups. While we utilized mixed-effects models to mitigate confounding factors in the comparative analysis, there may still be residual effects stemming from these differences. The mean dose of concomitant oral steroid was higher, and age was younger in the csDMARDs group. Steroid influence bone metabolism, and considering that most of our enrolled patients were female, age may have largely influenced the results of DXA via an influence of menopause. Furthermore, the disease phases differed, with a higher proportion of patients in earlier phases in the csDMARDs group. The dominant cytokines may vary by phase of disease progression; consequently, the inflammatory condition surrounding affected joints may differ.

In conclusion, this is the first study that investigated detailed changes of bone structure using HR-pQCT during abatacept treatment, with a comparison to csDMARDs. Our findings demonstrated that abatacept prevented progression of bone erosion, including new occurrence of bone erosion. Moreover, abatacept also prevented the worsening of bone strength. While statistical significance was not achieved in comparing abatacept to csDMARDs in terms of improvements in bone erosion and microarchitecture, the numerical trends favoring abatacept indicate its potential benefits. Specifically, abatacept demonstrated numerical improvements in bone erosion and mitigated the worsening of most parameters of bone microarchitecture compared to csDMARDs, suggesting its potential efficacy in inhibiting both bone erosion and microarchitectural deterioration.

Data availability

All data used in this study are available from the corresponding author upon request.

Received: 15 August 2024; Accepted: 22 October 2024

Published online: 12 November 2024

References

- van den Bergh, J. P. et al. The clinical application of high-resolution peripheral computed tomography (HR-pQCT) in adults: State of the art and future directions. *Osteoporos. Int.* **32**(8), 1465–1485 (2021).
- Peters, M. et al. Prospective Follow-up of cortical interruptions, bone density, and micro-structure detected on HR-pQCT: A study in patients with rheumatoid arthritis and healthy subjects. *Calcif. Tissue Int.* **104**(6), 571–581 (2019).
- Iwamoto, N. et al. Inhibition of bone erosion, determined by high-resolution peripheral quantitative computed tomography (HR-pQCT), in rheumatoid arthritis patients receiving a conventional synthetic disease-modifying anti-rheumatic drug (csDMARD) plus denosumab vs csDMARD therapy alone: An open-label, randomized, parallel-group study. *Arthritis Res. Ther.* **24**(1), 264 (2022).
- Figueiredo, C. P. et al. Bone erosion in the 2nd metacarpophalangeal head: Association with its bone mineral density by HR-pQCT in rheumatoid arthritis patients. *BMC Musculoskelet. Disord.* **22**(1), 109 (2021).
- Scharmga, A. et al. Structural damage and inflammation on radiographs or magnetic resonance imaging are associated with cortical interruptions on high-resolution peripheral quantitative computed tomography: A study in finger joints of patients with rheumatoid arthritis and healthy subjects. *Scand. J. Rheumatol.* **47**(6), 431–439 (2018).
- Finzel, S. et al. Comparison of the effects of tocilizumab monotherapy and adalimumab in combination with methotrexate on bone erosion repair in rheumatoid arthritis. *Ann. Rheum. Dis.* **78**(9), 1186–1191 (2019).
- Shimizu, T. et al. Assessment of 3-month changes in bone microstructure under anti-TNF α therapy in patients with rheumatoid arthritis using high-resolution peripheral quantitative computed tomography (HR-pQCT). *Arthritis Res. Ther.* **19**(1), 222 (2017).
- Simon, D. et al. Baricitinib improves bone properties and biomechanics in patients with rheumatoid arthritis: Results of the prospective interventional BARE BONE trial. *Arthritis Rheumatol.* **75**(11), 1923–1934 (2023).
- Schiff, M. et al. Head-to-head comparison of subcutaneous abatacept versus adalimumab for rheumatoid arthritis: Two-year efficacy and safety findings from AMPLE trial. *Ann. Rheum. Dis.* **73**(1), 86–94 (2014).
- Schiff, M. et al. Efficacy and safety of abatacept or infliximab vs placebo in ATTEST: A phase III, multi-centre, randomised, double-blind, placebo-controlled study in patients with rheumatoid arthritis and an inadequate response to methotrexate. *Ann. Rheum. Dis.* **67**(8), 1096–1103 (2008).
- Kerschbaumer, A. et al. Efficacy of synthetic and biological DMARDs: A systematic literature review informing the 2022 update of the EULAR recommendations for the management of rheumatoid arthritis. *Ann. Rheum. Dis.* **82**(1), 95–106 (2023).
- Kremer, J. M. et al. Long-term safety, efficacy and inhibition of radiographic progression with abatacept treatment in patients with rheumatoid arthritis and an inadequate response to methotrexate: 3-Year results from the AIM trial. *Ann. Rheum. Dis.* **70**(10), 1826–1830 (2011).

13. Westhovens, R. et al. Clinical efficacy and safety of abatacept in methotrexate-naïve patients with early rheumatoid arthritis and poor prognostic factors. *Ann. Rheum. Dis.* **68**(12), 1870–1877 (2009).
14. Tada, M. et al. Abatacept might increase bone mineral density at femoral neck for patients with rheumatoid arthritis in clinical practice: AIRTIGHT study. *Rheumatol. Int.* **38**(5), 777–784 (2018).
15. Chen, M. H. et al. Different effects of biologics on systemic bone loss protection in rheumatoid arthritis: An interim analysis of a three-year longitudinal cohort study. *Front. Immunol.* **12**, 783030 (2021).
16. Kim, K. W., Kim, H. R., Kim, B. M., Cho, M. L. & Lee, S. H. Th17 cytokines regulate osteoclastogenesis in rheumatoid arthritis. *Am. J. Pathol.* **185**(11), 3011–3024 (2015).
17. Aletaha, D. et al. 2010 Rheumatoid arthritis classification criteria: An American College of Rheumatology/European League Against Rheumatism collaborative initiative. *Arthritis Rheum.* **62**(9), 2569–2581 (2010).
18. Shiraishi, K. et al. Analysis of bone erosions in rheumatoid arthritis using HR-pQCT: Development of a measurement algorithm and assessment of longitudinal changes. *PLoS One.* **17**(4), e0265833 (2022).
19. Nishino, A. et al. Ultrasonographic efficacy of biologic and targeted synthetic disease-modifying antirheumatic drug therapy in rheumatoid arthritis from a multicenter rheumatoid arthritis ultrasound prospective cohort in Japan. *Arthritis Care Res.* **70**(12), 1719–1726 (2018).
20. Lassere, M. et al. OMERACT rheumatoid arthritis magnetic resonance imaging studies. Exercise 3: An international multicenter reliability study using the RA-MRI Score. *J. Rheumatol.* **30**(6), 1366–1375 (2003).
21. Ostergaard, M. et al. An introduction to the EULAR-OMERACT rheumatoid arthritis MRI reference image atlas. *Ann. Rheum. Dis.* **64**(Suppl 1), i3–7 (2005).
22. van der Heijde, D. How to read radiographs according to the Sharp/van der Heijde method. *J. Rheumatol.* **26**(3), 743–745 (1999).
23. Koga, T. et al. Prognostic factors toward clinically relevant radiographic progression in patients with rheumatoid arthritis in clinical practice: A Japanese multicenter, prospective longitudinal cohort study for achieving a treat-to-target strategy. *Medicine* **95**(17), e3476 (2016).
24. Iwamoto, N. et al. Association of denosumab with serum cytokines, chemokines, and bone-related factors in patients with rheumatoid arthritis: A post hoc analysis of a multicentre, open-label, randomised, parallel-group study. *Mod. Rheumatol.* **34**, 936–946 (2024).
25. Klose-Jensen, R. et al. Diagnostic accuracy of high-resolution peripheral quantitative computed tomography and X-ray for classifying erosive rheumatoid arthritis. *Rheumatology* **61**(3), 963–973 (2022).
26. Adami, G. et al. Changes in bone turnover markers and bone modulators during abatacept treatment. *Sci. Rep.* **13**(1), 17183 (2023).
27. Roser-Page, S. et al. CTLA-4Ig (abatacept) balances bone anabolic effects of T cells and Wnt-10b with antianabolic effects of osteoblastic sclerostin. *Ann. N.Y. Acad. Sci.* **1415**(1), 21–33 (2018).
28. Hoff, M., Haugeberg, G. & Kvien, T. K. Hand bone loss as an outcome measure in established rheumatoid arthritis: 2-Year observational study comparing cortical and total bone loss. *Arthritis Res. Ther.* **9**(4), R81 (2007).
29. Deodhar, A. A., Brabyn, J., Pande, I., Scott, D. L. & Woolf, A. D. Hand bone densitometry in rheumatoid arthritis, a five year longitudinal study: An outcome measure and a prognostic marker. *Ann. Rheum. Dis.* **62**(8), 767–770 (2003).
30. Guler-Yuksel, M. et al. Changes in hand and generalised bone mineral density in patients with recent-onset rheumatoid arthritis. *Ann. Rheum. Dis.* **68**(3), 330–336 (2009).
31. Bozec, A. et al. T cell costimulation molecules CD80/86 inhibit osteoclast differentiation by inducing the IDO/tryptophan pathway. *Sci. Transl. Med.* **6**(235), 235RA60 (2014).
32. Okada, H. et al. CTLA4-Ig directly inhibits osteoclastogenesis by interfering with intracellular calcium oscillations in bone marrow macrophages. *J. Bone Miner. Res.* **34**(9), 1744–1752 (2019).
33. Matsuura, Y. et al. In vivo visualisation of different modes of action of biological DMARDs inhibiting osteoclastic bone resorption. *Ann. Rheum. Dis.* **77**(8), 1219–1225 (2018).
34. Adam, S. et al. JAK inhibition increases bone mass in steady-state conditions and ameliorates pathological bone loss by stimulating osteoblast function. *Sci. Transl. Med.* **12**(530), 4447 (2020).
35. Komagamine, M. et al. Effect of JAK inhibitors on the three forms of bone damage in autoimmune arthritis: Joint erosion, periarticular osteopenia, and systemic bone loss. *Inflamm. Regen.* **43**(1), 44 (2023).
36. So, H. et al. Effects of RANKL inhibition on promoting healing of bone erosion in rheumatoid arthritis using HR-pQCT: A 2-year, randomised, double-blind, placebo-controlled trial. *Ann. Rheum. Dis.* **80**(8), 981–988 (2021).
37. Conaghan, P. G. et al. Impact of intravenous abatacept on synovitis, osteitis and structural damage in patients with rheumatoid arthritis and an inadequate response to methotrexate: The ASSET randomised controlled trial. *Ann. Rheum. Dis.* **72**(8), 1287–1294 (2013).
38. Kaine, J. et al. Evaluation of abatacept administered subcutaneously in adults with active rheumatoid arthritis: Impact of withdrawal and reintroduction on immunogenicity, efficacy and safety (phase IIb ALLOW study). *Ann. Rheum. Dis.* **71**(1), 38–44 (2012).
39. Wells, A. F. et al. Abatacept plus methotrexate provides incremental clinical benefits versus methotrexate alone in methotrexate-naïve patients with early rheumatoid arthritis who achieve radiographic nonprogression. *J. Rheumatol.* **38**(11), 2362–2368 (2011).
40. Forsprecher, J., Wang, Z., Goldberg, H. A. & Kaartinen, M. T. Transglutaminase-mediated oligomerization promotes osteoblast adhesive properties of osteopontin and bone sialoprotein. *Cell Adh. Migr.* **5**(1), 65–72 (2011).
41. Marycz, K. et al. Nanohydroxyapatite (nHAp) doped with iron oxide nanoparticles (IO), miR-21 and miR-124 under magnetic field conditions modulates osteoblast viability, reduces inflammation and inhibits the growth of osteoclast: A novel concept for osteoporosis treatment: Part 1. *Int. J. Nanomed.* **16**, 3429–3456 (2021).
42. Lei, C., Xueming, H. & Ruihang, D. MLN64 deletion suppresses RANKL-induced osteoclastic differentiation and attenuates diabetic osteoporosis in streptozotocin (STZ)-induced mice. *Biochem. Biophys. Res. Commun.* **505**(4), 1228–1235 (2018).
43. Bernards, M. T., Qin, C., Ratner, B. D. & Jiang, S. Adhesion of MC3T3-E1 cells to bone sialoprotein and bone osteopontin specifically bound to collagen I. *J. Biomed. Mater. Res. A* **86**(3), 779–787 (2008).
44. Walker, C. G., Dangaria, S., Ito, Y., Luan, X. & Diekwisch, T. G. Osteopontin is required for unloading-induced osteoclast recruitment and modulation of RANKL expression during tooth drift-associated bone remodeling, but not for super-eruption. *Bone* **47**(6), 1020–1029 (2010).
45. Lv, Q. et al. The status of rheumatoid factor and anti-cyclic citrullinated peptide antibody are not associated with the effect of anti-TNF α agent treatment in patients with rheumatoid arthritis: A meta-analysis. *PLoS One* **9**(2), e89442 (2014).
46. Harrold, L. R. et al. Baseline anti-citrullinated protein antibody status and response to abatacept or non-TNF α biologic/targeted-synthetic DMARDs: US observational study of patients with RA. *Rheumatol. Ther.* **9**(2), 465–480 (2022).

Acknowledgements

We thank Mami Ushiroda for data collection.

Author contributions

N.I.: Conception and design of the study, analysis and interpretation of data and drafting of the article. K.C.: Conception and design of the study, analysis and interpretation of HR-pQCT data. N.I., S.S.: Statistical analysis and interpretation of data. K.C., K.S., K.W., N.O.: Analysis and interpretation of HR-pQCT data. S.T.: Collection

and assembly of data. N.I., N.O., A.O., T.K., S.K., M.T.: Analysis and interpretation of MRI, US and X-ray data. N.I., K.C., S.S., K.S., K.W., N.O., A.O., T.K., S.K., M.T., M.O., A.K.: Analysis and interpretation of data, critical revision of the manuscript. A.K.: Project supervision. All authors have given their final approval of the manuscript to be published as presented.

Funding

This study was supported by Bristol-Myers Squibb K.K. and Ono Pharmaceutical Co. Ltd.

Declarations

Competing interests

Naoki Iwamoto and Atsushi Kawakami have received grant research support from Ono Pharmaceutical Co. Ltd and Bristol-Myers Squibb K.K.

Ethical approval and consent to participate

This study was performed in accordance with the Declaration of Helsinki and was approved by the Investigation and Ethics Committee at Nagasaki University. Patients gave their informed consent to be subjected to the protocol.

Additional information

Supplementary Information The online version contains supplementary material available at <https://doi.org/10.1038/s41598-024-77392-9>.

Correspondence and requests for materials should be addressed to N.I.

Reprints and permissions information is available at www.nature.com/reprints.

Publisher's note Springer Nature remains neutral with regard to jurisdictional claims in published maps and institutional affiliations.

Open Access This article is licensed under a Creative Commons Attribution-NonCommercial-NoDerivatives 4.0 International License, which permits any non-commercial use, sharing, distribution and reproduction in any medium or format, as long as you give appropriate credit to the original author(s) and the source, provide a link to the Creative Commons licence, and indicate if you modified the licensed material. You do not have permission under this licence to share adapted material derived from this article or parts of it. The images or other third party material in this article are included in the article's Creative Commons licence, unless indicated otherwise in a credit line to the material. If material is not included in the article's Creative Commons licence and your intended use is not permitted by statutory regulation or exceeds the permitted use, you will need to obtain permission directly from the copyright holder. To view a copy of this licence, visit <http://creativecommons.org/licenses/by-nc-nd/4.0/>.

© The Author(s) 2024